Link Scheduling for Data Collection in SIC-Capable UAV Networks

Yawen Zheng and Kwan-Wu Chin
School of Electrical, Computer and Telecommunications Engineering
University of Wollongong, NSW, Australia
Email: yz757@uowmail.edu.au, kwanwu@uow.edu.au

***Abstract*—Unmanned Aerial Vehicles (UAVs) are ideal as aerial base stations, mobile relays or data collectors. In this paper, we consider a UAV with a Successive Interference Cancellation (SIC) radio that visits M collection points to download data from ground devices or sensors. The problem at hand is to determine the links to be scheduled at each data collection point. To this end, we formulate an Integer Linear Program (ILP) to compute the optimal transmission schedule. We also propose a Cross-Entropy (CE) approach to select links when there are a large number of ground devices. Our results show that SIC helps double the amount of data collected by the UAV. We also find that the average throughput is affected by the number of ground devices and the number of data collection points. Lastly, our CE approach is capable of producing a schedule that is near optimal.**

1. Introduction

To date, researchers have employed a variety of mobile vehicles to augment existing communication infrastructures [1]. The benefits of mobile vehicles such as Unmanned Aerial Vehicles (UAVs) include (i) better coverage and capacity enhancement, especially for users located far from a base station [2], (ii) prolonging the lifetime of Wireless Sensor Networks (WSNs) [3], and (iii) serving as a platform that can be used to offload traffic or computation [4]. In addition, mobile vehicles can fly periodically over sensors and Internet of Things (IoTs) to collect/deliver data.

One approach to improve the amount of data collected by a UAV is to employ Multi-Packet Reception (MPR) technologies such as Successive Interference Cancellation (SIC) [5]; indeed, SIC is part of Non-Orthogonal Multiple Access (NOMA) and is a key 5G technology. A UAV equipped with a SIC radio is thus able to decode multiple simultaneous transmissions subject to these transmissions meeting Signal-to-Interference-Plus-Noise Ratio (SINR) conditions. To this end, we consider a single-hop UAV network comprising of multiple ground devices and a SIC-capable UAV. The UAV collects data from these ground devices at multiple data collection points. Critically, it takes advantage of the different channel gain or received power from each ground device at each collection point to construct a schedule that yields the maximum throughput.

To illustrate our problem, consider the example given in Figure 1. We see two data collection point ξ_1 and ξ_2 as well as four ground devices: A, B, C, D. The UAV flies from left to right. At each collection point, the UAV needs to decide the transmitting ground devices. One possible schedule at ξ_1 is for A and D to transmit concurrently. This assumes the received power of both these devices meets SIC condition; see Section 2. Another possible schedule consists of ground devices B and C; their uplink is denoted by a black dotted line. Thus, at collection point ξ_1, we have two link schedules: $\{A, D\}$ and $\{B, C\}$. At collection point ξ_2, there are two schedules: $\{A, B, C\}$ or $\{D\}$. The problem at hand is to choose $\{A, D\}$ or $\{B, C\}$ at ξ_1, and either $\{A, B, C\}$ or $\{D\}$ at ξ_2. The chosen schedule must maximize throughput over these two data collection points.

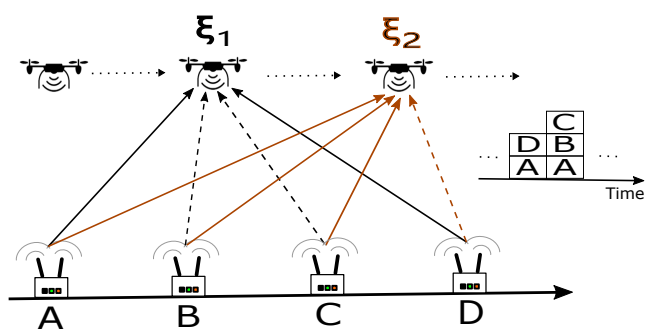

Figure 1. An example UAV network. Different patterns indicate uplinks belong to different link schedules.

To date, many papers have considered computing the optimal trajectory of one or more UAVs. In [6] and [7], the authors study downlinks between UAV(s) and ground terminals. In both works, the communication between the UAV and ground terminals are scheduled in a cyclical time-division manner. The aim of [6] is to maximize the minimum throughput of ground terminals by determining the time allocation of each terminal. The authors of [7] also aim to optimize the UAV's trajectory and transmit power control. Additionally, reference [7] studies a multi-hop wireless network. However, these works do not aim to derive a link schedule nor consider UAVs equipped with a SIC radio. Past works on SIC consider (i) static transmitter(s) and receiver(s), (ii) a fixed channel gain, and (iii) one time slot. For example, in [8] and [9], the authors study link scheduling in scenarios with multiple pairs of transmitters

and receivers. The authors of [8] aim to construct a schedule and link data rate that maximizes SIC and Parallel Interference Cancellation (PIC). In [9], the authors partition active transmitters into groups and determine the receiver that have minimal interference. Moreover, they ensure links in each group have sufficient SINR in each stage of the SIC decoding process. However, these works are not designed for a mobile node, and do not seek to take advantage of the different channel gain when the mobile node is located at different positions/locations. Moreover, they do not aim to optimize data collection over a finite time horizon. In [10], the authors aim to optimize SIC and Mobile Base Stations (MBSs) movement to minimize a MBS's data collection time by identifying good data collection points. However, the work in [10] is not focused on generating a link schedule that maximizes the amount of collected data.

Unlike prior works, this paper makes the following contributions: (i) we consider a new problem, where we seek to derive a schedule over M data collection points that yields the highest average throughput. A key distinction of our work is that we take advantage of the different channel gains of ground devices at each collection point to maximize SIC decoding success, (ii) we outline a Integer Linear Program (ILP) that can be used to solve the problem at hand, (iii) we apply the Cross-Entropy (CE) method [11] to derive a solution for large scale networks, (iv) our results show that with a SIC radio, the UAV is able to collect more data. Moreover, they show that the average throughput is effected by the number of ground devices and the number of data collection points. Specifically, with more ground devices, the average throughput will increase. This is because more ground devices yield larger possible link schedules. On the contrary, the average throughput decreases with more data collection points.

Next, we define our notations in Section 2 before presenting our ILP model in Section 3. After that, in Section 4, we show how the CE method can be used to compute the solution for large scale networks. Then in Section 5, we present our results. Section 6 concludes the paper.

2. Preliminaries

We consider a single-hop wireless system consisting of multiple ground devices and a mobile SIC-capable UAV. Let $\mathbf{G}$ be the set of ground devices, where $G = |\mathbf{G}|$. We index these ground devices as $1, 2, \ldots, G$. We assume ground devices are spaced equally along a straight line with a length of d meters. The first ground device, aka g_1, is set as the origin. Also, these ground devices are saturated, meaning they always have data to transmit.

The UAV u flies horizontally at a fixed altitude h and is used to collect data from ground devices. The UAV moves with a constant speed s and is initially located above ground device g_1. We assume that the UAV collects data from ground devices at M data collection points to guarantee all ground devices have any opportunity to upload their data [12]. In particular, a ground station may have a link to the UAV at one or more data collection points. Let $\mathbf{M}$ be the set of data collection points, where $m \in \mathbf{M}$ and $M = \mathbf{M}$. We index these collection points as $1, 2, \ldots, M$, and assume at each collection point m, each ground device i has one uplink that is denoted as l_i^m. Let L^m be a set that consists of all uplinks at collection point m, where $L^m = \{l_i^m\}, m \in \mathbf{M}, i \in \mathbf{G}$. We use r_i^m to denote the data rate of uplink l_i^m at collection point m.

The path loss of uplinks from ground device i to the UAV at collection point m is denoted as $\mathcal{P}(d_i^m)$ (dBm). We assume block fading where a channel remains constant within each time slot but varies across multiple time slots. The path loss is calculated by

$$\mathcal{P}(d_i^m) = \mathcal{P}(d_0) + 10\alpha \log_{10} \frac{d_i^m}{d_0} + \mathcal{N}(\mu, \sigma^2) \qquad (1)$$

where d_i^m is the Euclidean distance from the collection point m to ground device i, d_0 is the reference distance, $\mathcal{P}(d_0)$ (in dBm) is the path loss at the reference distance, and α is the path loss exponent. The Gaussian random variable, denoted as $\mathcal{N}(\mu, \sigma^2)$, has mean $\mu = 0$ and variance σ_g^2. We assume all ground devices have a fixed transmit power P (dBm). The received power (in Watt) from ground device i when the UAV is at data collection point m is,

$$P_i^m = 10^{\frac{P - \mathcal{P}(d_i^m)}{10}} \qquad (2)$$

The UAV has a SIC radio [5] that is capable of decoding up to L_{max} simultaneous uplink transmissions. In particular, it separates, decodes, and removes signals from a composite signal in multiple stages. It first decodes the strongest received signal. It then removes the decoded signal from the composite signal and repeats the process until all signals are decoded. To ensure decoding success, it is important that the received power of each uplink is sufficiently different. As an example, assume UAV u is receiving from G ground devices simultaneously, where $i \in \mathbf{G}$. Assume the received power at the UAV u is in non-decreasing order: $P_1 \leq P_2 \leq \cdots \leq P_G$. The decoding order is thus $G, G-1, \ldots, 2, 1$. That is, the signal with received power P_G can be decoded if and only if all the preceding stronger signals are first decoded and removed. Formally, we have,

$$\begin{array}{ll} \text{Stage 1} & \dfrac{P_G}{N_0 + \sum_{i=1}^{G-1} P_i} \geq \beta \\ \text{Stage 2} & \dfrac{P_{G-1}}{N_0 + \sum_{i=1}^{G-2} P_i} \geq \beta \\ \vdots & \vdots \\ \text{Stage (G-q+1)} & \dfrac{P_{q\varphi}}{N_0 + \sum_{i=1}^{q-1} P_i} \geq \beta \end{array} \qquad (3)$$

We see that for a given uplink, its Signal-to-Interference-Noise Ratio (SINR) and/or Signal-to-Noise Ratio (SNR) must be no less than the threshold value β, which corresponds to a given Modulation and Coding Scheme (MCS). In (3), N_0 denotes the ambient noise power.

3. Problem Definition

Our problem is to find the optimal schedule that maximizes the total uploaded data from ground devices to a SIC-capable UAV. In particular, we need to decide the links that are activated at each collection point. In particular, we aim to exploit the difference in received power at data collection points to maximize SIC decoding success, and thus the total sum-rate over all M collection points.

We require the following notations to formalize our problem. At each collection point, there are multiple link sets. Each link set contains one or more uplinks from ground stations, and critically they satisfy SIC constraints; i.e., (3). At each point m, we define a collection $\mathbf{C^m}$ of link sets. Each link set is denoted as C_j^m, where $j \in \{1, |\mathbf{C^m}|\}$, and $C_j^m \subseteq L^m$. The maximum number of concurrent uplinks in each link set C_j^m is set to L_{max}, which is a technological limit that corresponds to the maximum number signals that can be cancelled by a SIC radio [5]. The sum-rate of link set C_j^m is denoted as r_j^m, and is defined as, $R_j^m = \sum_{i \in G} r_i^m$. As an example, consider Figure 2; there is one UAV u and three ground devices g_1, g_2 and g_3. We denote each data collection point as $\xi_m, m \in \{1, \ldots, M\}$. We use a different color to indicate uplinks at each data collection point ξ_m and use a different pattern to indicate uplinks from different link sets C_j^m. At collection point ξ_1, there are two link sets $C_1^1 = \{l_1^1, l_2^1\}$ and $C_2^1 = \{l_2^1, l_3^1\}$. All three uplinks can transmit concurrently at point ξ_2 and the corresponding link set is $C_1^2 = \{l_1^2, l_2^2, l_3^2\}$. The two link sets at ξ_M are $C_1^M = \{l_1^M, l_2^M\}$ and $C_2^M = \{l_3^M\}$. Given these links sets, we aim to choose one link set from each collection point that yields the maximum sum-rate over M data collection points. For example, one solution is $\{C_1^1, C_1^2, \ldots, C_2^M\}$, with a corresponding sum-rate of $r_1^1 + r_2^1 + r_1^2 + r_2^2 + r_3^2 + \cdots + r_3^M$.

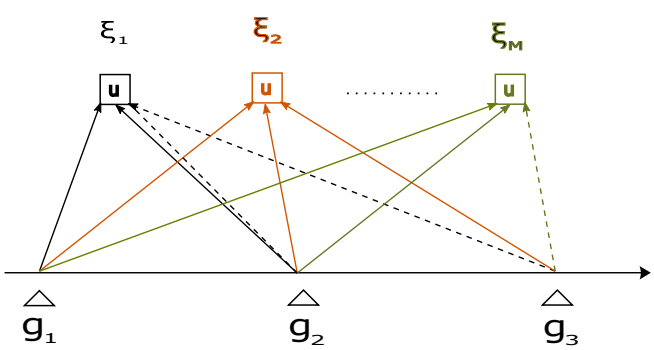

Figure 2. Example links at M collection points

Next, we present an Integer Linear Program (ILP) to compute a schedule that maximizes the sum-rate over M data collection points, see (4). The ILP has one binary decision variable x_j^m that indicates whether the link set C_j^m is active ($x_j^m = 1$) at data collection point m. The indicator function $\delta(C_j^m, i)$ indicates whether ground device i is in the link set C_j^m ($\delta(C_j^m, i) = 1$) at collection point m. Mathematically, we have the following ILP:

$$\max \quad \sum_{m \in \mathbf{M}} \sum_{j=1}^{|\mathbf{C^m}|} R_j^m x_j^m \tag{4a}$$

s.t.

$$\sum_{m \in \mathbf{M}} \sum_{j=1}^{|\mathbf{C^m}|} \delta(C_j^m, i) x_j^m \geq 1 \ \forall i \in \mathbf{G} \tag{4b}$$

$$\sum_{j=1}^{|\mathbf{C^m}|} x_j^m = 1 \qquad \forall m \in \mathbf{M} \tag{4c}$$

$$x_j^m \in \{0, 1\} \qquad \forall m \in \mathbf{M}, \forall j \in \mathbf{C^m} \tag{4d}$$

Constraint (4b) ensures each ground device is included in the derived schedule. At each data collection point m, constraint (4c) ensures there is only one active set cover. Lastly, constraint (4d) specifies that the corresponding variable is binary.

4. A Cross-Entropy (CE) Method

The formulated ILP can only be used to solve small problem instances; note that link scheduling in general is an NP-hard problem [13]. Thus, for larger problem instances, we resort to a heuristic based on the CE method; interested readers are referred to [11] for more information. CE is an iterative method. It has the following steps: in each iteration, (i) it generates Z random transmission schedules, aka samples, according to a Probability Mass Function (PMF), (ii) it then determines the reward of each sample z_k, where $k = 1, \ldots, Z$. In our case, the reward of each sample corresponds to the throughput of a sample or schedule over M collection points, (iii) with Z rewards in hand, it identifies so called "elite" samples. That is, it sorts the reward of Z samples in non-decreasing order. Given a threshold $\gamma \in [0, 1]$, it then identifies the $(1 - \gamma)$-th quantile reward value, which is denoted as φ. Then CE method then collects the samples with a reward value that satisfies $r_k \geq \varphi$, and stores them in a vector called Z^*, and (iv) lastly, it uses these elite samples to improve the PMF used in step (i) so as to obtain better samples in the next iteration. The foregone four steps repeat until the PMF converges.

We now make specific the definition of a sample. For each sample z_k, there are $N = |G| \times |M|$ binary variable x_i^m, where we have $x_i^m = 1$ when the ground device i is active at data collection point m. Let $X^m \in \{0, 1\}^{|G|}$ be a binary vector that indicates the link set at collection point m. Hence, a schedule or sample is defined as $z_k = (X^1, X^2, \ldots, X^{|M|})$. The sum-rate of each link set X^m is r^m. Therefore, we have $r_k = (r^1, r^2, \ldots, r^{|M|})$. Each sample z_k is characterized by a multivariate Bernoulli distribution $f(z_k; V^c)$, i.e., $z_k \sim Ber(\mathbf{p}^r)$. The real-valued parameter (vector) $V^c \in [0, 1]^N$ describes the success/failure probability of each item x_i^m in z_k at iteration c. Initially, at iteration $c = 1$, we assume all ground devices have equal probability of being selected or not selected at each

collection point; i.e., $V^1 = (0.5, 0.5, \dots)$. We define the parameter ρ as a smoothing parameter that determines how fast the probabilities in V^c converge. We denote the n-th element in V^c as V^c_n.

Referring to Algorithm 1, in line 2-5, we use V^1 to generate Z samples, and then proceed to calculate the reward of each sample using the function $\mathcal{R}(.)$; see Algorithm 2. Specifically, Algorithm 2 iterates through the link set at each collection point and determine the sum-rate of each sample z_k. It checks whether SIC is successful for all links in set X^m in sample z_k, see line 4. Assume the received power P^m_i of the G ground devices are in decreasing order; formally, $P^m_i \geq P^m_{i+1} \geq \dots \geq P^m_G$. The decoding order at the UAV u is thus $1, 2, \dots, G-1, G$. If the SINR of ground device i exceeds β, then we add its data rate to the sum r^m. In line 11, Algorithm 2 sums the reward of all link sets and returns the reward r_k of sample z_k.

Referring to Algorithm 1, in line 6 of Algorithm 1, it sorts the rewards in non-decreasing order; denote the sorted list as $\mathbf{R}$. Then line 7 uses φ^c as the cut-off reward threshold to identify elite samples; i.e., a value that is in the $(1-\gamma)$-th percentile of $\mathbf{R}$. In line 8-9, we update the probabilities in V^c and use the updated PMF to generate Z new samples for the next iteration. The probability of each item n in PMF V^c is computed via

$$V^c_n = \frac{\sum_{k=1}^{Z} \mathbb{1}_{\{\mathbf{r}_k \geq \varphi^c\}} \mathbb{1}_{\{z_{kn}=1\}}}{\sum_{k=1}^{Z} \mathbb{1}_{\{\mathbf{r}_k \geq \varphi^c\}}} \tag{5}$$

Here $\mathbb{1}_a$ is an indicator function that returns a value of one if the condition a is true. Equ. (5) counts how many times each item is active among all elite samples/schedules. Specifically, the denominator of Equ. (5) is the total number of elite samples. The numerator corresponds to the total number of times that the n-th item occurs in the elite samples. Note that instead of updating the PMF directly, we use a smoothed version that considers the influence of past values V^{c-1}, see line 10. This allows the CE-method to explore more samples before converging onto the best schedule. Lastly, we conclude that CE has converged when the probability V^c of selecting a ground device in each slot is within a certain tolerance θ away from one or zero.

Algorithm 1: CE method based link scheduler

Initialize: $V^1 = [0.5, \dots, 0.5], c = 1, \gamma, \delta$
1 **while** *not Converge(V^c)* **do**
2 **for** $k \leftarrow 1$ *to* Z **do**
3 z_k = $\mathcal{Z}(V^c)$;
4 r_k = $\mathcal{R}(z_k)$;
5 **end**
6 $\mathbf{R}$ = Sort $(r_1, \dots, r_Z)$;
7 φ^c = Percentile($(1-\gamma), \mathbf{R}$) ;
8 **for** $n \leftarrow 1$ *to* $|V^c|$ **do**
9 V^c_n = $\rho V^c_n + (1-\rho) V^{c-1}_n$;
10 **end**
11 $c \leftarrow c + 1$;
12 **end**

Algorithm 2: The sum-rate of a sample.

input : z_k
output: r_k
1 **for** $m \leftarrow 1$ *to* M **do**
2 $r^m = 0$
3 **for** $i \leftarrow 1$ *to* G **do**
4 **for** $g \leftarrow i+1$ *to* G **do**
5 **if** $\frac{P^m_i}{N_0 + \sum_g^G P^m_g} \geq \beta$ **then**
6 $r^m = r^m + r^m_i$
7 **else**
8 break
9 **end**
10 **end**
11 **end**
12 r_k = $\sum_m^M r^m$
13 **end**

5. Evaluation

We conduct our experiments in Matlab. Our system consists of up to ten ground devices. We assume the UAV has a known trajectory and it takes 100 seconds to visit all ten collection points; this means it collects data every 10 seconds. We use the SINR and data rate mapping from Cisco [14]. We record the resulting data rate, where a transmission is successful if its SINR and/or SNR exceeds $\beta = 5$ (dB). We run each simulation 50 times and plot the average results. The simulation settings are listed in Table 1. We compare the results from solving the formulated ILP, labeled as SIC-ILP, with three other methods: (i) CE, (ii) Slotted Aloha, and (iii) TDMA. Additionally, we test our CE method against both fixed and adaptive cut-off reward threshold φ^c, which we label as *CE Fixed* φ^c and *CE Adaptive* φ^c, respectively.

1. Basic system settings				
Symbol	G	M	u	L_{max}
Value	10	10	1	4
2. UAV and ground devices deployment				
Symbol	d	h	s	P
Value	300m	100m	26 m/s	1 W
3. SNR and SINR calculation				
Symbol	α	β	N_0	σ^2
Value	2.7	5 dB	-90 dBm	2 dB^2

TABLE 1. SYSTEM SETTINGS

From Figure 3(a), we see that SIC-ILP outperforms the other four methods because it is able to find the optimal link setsat each data collection point that leads to the maximal average throughput. For example, in case of ten ground devices, the average data rate is approximately 12.6 Mbps. However, CE Adaptive φ^c and CE Fixed φ^c achieve 8.9 Mbps and 8.5 Mbps, respectively, for the same number of ground devices. The average throughput for TDMA and Slotted Aloha is only 5.4 Mbps and 3.8 Mbps, respectively. Referring to Figure 3(a), we find that with increasing

number of ground devices, the average throughput of SIC-ILP and Slotted Aloha increases. This is because more ground devices provide larger possible link sets at each collection point. Therefore, when there are many ground devices, the chance to activate link sets with better sum-rate increases, which results in a higher throughput. The average throughput for TDMA is fixed at 5.4 Mbps for any number of ground devices because it allows only one active uplink in each time slot.

From Figure 3(a), we also find that the average throughput for CE Adaptive φ^c and CE Fixed φ^c first increases and then decreases. Specifically, the average throughput increases about 4.5 Mbps when there are one to eight ground devices. The average throughput then decreases from 9.9 Mbps to 8.9 Mbps when the number of ground devices increases from eight to ten. Moreover, the average throughput starts to decrease when there are more than six ground devices. The is due to SIC's decoding limit, which restricts the number of uplinks per link set to be no more than L_{max} [5]. Apart from that, with more ground devices, the received power difference of active active links will be smaller, which lead to low SINR. Therefore, the individual link rate will be smaller, which decreases the sum-rate.

Next, we study the impact of the number of data collection points M on both the average throughput and throughput fairness of ground devices by using the CE method. The CE Adaptive φ^c method yields the same trend as CE Fixed φ^c method. Thus, we only plot the results of the CE Fixed φ^c method. We consider the following G values: 1, 3, 6 and 10. The number of data collection points M is increased from one to ten. The smoothing paramet ρ is set to 0.7 and the cut-off reward identify parameter γ is fixed at 0.95. The tolerance bound θ that use to detect convergence is 10^2. In each CE iteration, we generate 100 samples.

Figure 3(b) shows the average throughput with increasing number of data collection points. From Figure 3(b), we see that when there are multiple ground devices, the average throughput is around twice that of the case with one ground device. Specifically, when there is only one ground device, the average throughput remains constant at 5.4 Mbps. The reason is that SIC allows multiple links to transmit concurrently. However, if there is only one ground device, SIC does not take effect and signals are decoded one by one as TDMA. For cases with three, six and ten ground devices, the average throughput decreases with increasing number of data collection points. For example, when there is only one collection point, the average throughput of three cases are 10.2 Mbps, 12 Mbps and 13.6 Mbps, respectively. However, when there are ten data collection points, the average throughput becomes 6.8 Mbps, 8.5 Mbps and 8.2 Mbps, respectively. This is because of SIC's decoding limit that restricts the number of concurrent active uplinks. Additionally, the data rate of each uplink is determined by the individual SNR and/or SINR value after successful SIC decoding. Therefore, when the number of collection points increases, the total transmitted data will not have equal increases. Specifically, we use the average throughput to show the rate of data transmission that is computed by the total transmitted data dividing the total time slots. If the total transmitted data does not increase with equal proportion, the average throughput will decrease. Additionally, we find that when there are more than five collecting points, the average throughput of ten ground devices case is 0.3 Mbps smaller than that of six ground devices case. The reason is that the number of concurrent uplinks cannot exceed the upper bound L_{max} that SIC can support. When there are ten ground devices and the schedule length has more than five slots, there may be more than five active links at each collection point, which lead to decoding failures. Consequently, the corresponding reward will be smaller.

Next, we study how different number of collection points and number of ground devices affect fairness; see Figure 3(c). We use Jains Fairness index (JFi) [15] to judge whether each ground device has equal opportunity to communicate with the UAV. Specifically, JFi reflects whether each ground device transmits equal amount of data. Figure 3(c) shows the change in JFi for four different number of ground devices case when we increase the number of data collection points. Referring to Figure 3(c), we see the JFi of one ground device is a constant value at one. Specifically, the single ground device can always transmit the same amount of data at each collection point. Moreover, we find that the JFi decreases with the increasing number of ground devices. For example, when there are three collection points, the JFi of three, six and ten ground devices case is 0.8, 0.65 and 0.5, respectively. The reason is that when there are a large number of ground devices, the SIC's decoding limit will cause the UAV takes long to active all ground devices. Therefore, the transmitted data of each ground device is unequal; hence, the JFi will be smaller.

In Figure 3(c), we see that when the number of data collection points is smaller than the number of ground devices, the JFi will increase. The reason is that under this circumstance, the multiple positions of the moving UAV is large enough to (i) allow each of the ground devices to transmit at least once, and (ii) allow SIC decoding to be successful. Thus, the data transmission of each ground device is more homogeneous. However, when the number of data collection points is bigger than the number of ground device, the location of the UAV is far away from the last ground device and the UAV will not be in the coverage of ground devices. Moreover, SIC is preferable when the received power levels are different. Therefore, ground devices that are the closest to the UAV and located far away from the UAV have higher opportunity to be active. Consequently, the amount of transmitted data from each ground device is unequal; hence, the value of JFi drops.

6. Conclusion

This paper has studied a novel problem involving a mobile UAV equipped with a SIC radio that collects data from ground devices. We formulate an ILP that can be used to derive a link schedule that maximizes the total uploaded data. We also propose a cross-entropy based method to solve large problem instances. Our results indicate that the use of

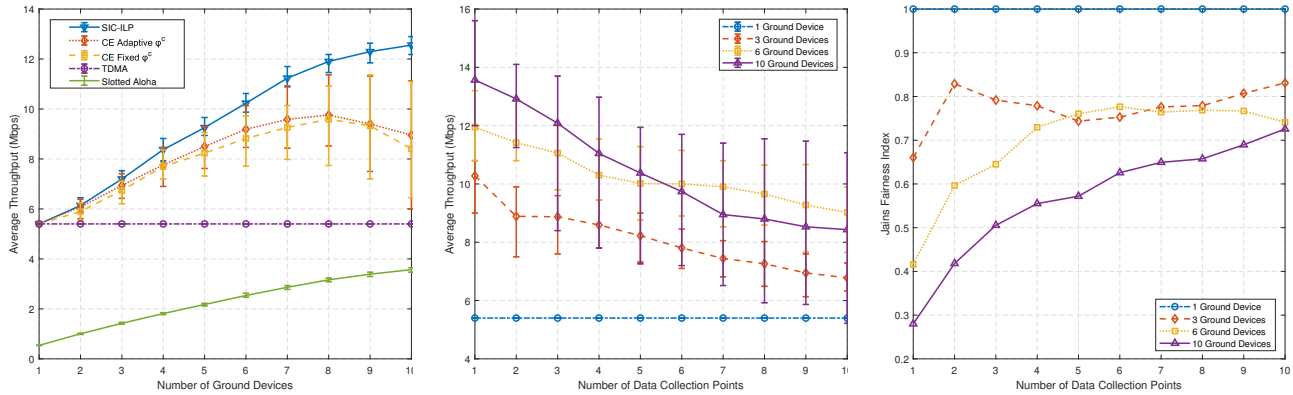

(a) (b) (c)

Figure 3. Performance of SIC-ILP and CE Fixed φ^c. (a) SIC-ILP, CE Fixed φ^c, CE Adaptive φ^c, slotted Aloha and TDMA comparison, (b) average throughput of CE Fixed φ^c, and (c) Jain's fairness index of CE Fixed φ^c.

SIC helps double the amount of collected data by the UAV. Additionally, our results indicate that the average throughput decreases as the number of data collection points increases. This is because of the SIC's decoding limit that restricts the number of concurrent active uplinks. Also they indicate the number of ground devices and data collection points are jointly affect the fairness of ground device. A future work will be to design the location of data collection points.

References

[1] N. H. Motlagh, T. Taleb, and O. Arouk, "Low-altitude unmanned aerial vehicles-based internet of things services: Comprehensive survey and future perspectives," *IEEE Internet of Things Journal*, vol. 3, no. 6, pp. 899–922, Dec. 2016.

[2] Y. Zeng, R. Zhang, and T. J. Lim, "Throughput maximization for UAV-enabled mobile relaying systems," *IEEE Transactions on Communications*, vol. 64, no. 12, pp. 4983–4996, Dec. 2016.

[3] M. Di Francesco, S. K. Das, and G. Anastasi, "Data collection in wireless sensor networks with mobile elements: A survey," *ACM Transactions on Sensor Networks (TOSN)*, vol. 8, no. 1, p. 7, 2011.

[4] Y. Zeng, R. Zhang, and T. J. Lim, "Wireless communications with unmanned aerial vehicles: Opportunities and challenges," *IEEE Communications Magazine*, vol. 54, no. 5, pp. 36–42, 2016.

[5] D. Halperin, T. Anderson, and D. Wetherall, "Taking the sting out of carrier sense: Interference cancellation for wireless lans," in *ACM MOBICOM*, San Francisco, CA, USA, 2008, pp. 339–350.

[6] J. Lyu, Y. Zeng, and R. Zhang, "Cyclical multiple access in uav-aided communications: A throughput-delay tradeoff," *IEEE Wireless Communications Letters*, vol. 5, no. 6, pp. 600–603, Dec 2016.

[7] Q. Wu, Y. Zeng, and R. Zhang, "Joint trajectory and communication design for multi-uav enabled wireless networks," *IEEE Trans. on Wirel. Comms*, vol. 17, no. 3, pp. 2109–2121, March 2018.

[8] V. Angelakis, L. Chen, and D. Yuan, "Optimal and collaborative rate selection for interference cancellation in wireless networks," *IEEE Communications Letters*, vol. 15, no. 8, pp. 819–821, Aug. 2011.

[9] Q. He, D. Yuan, and A. Ephremides, "Maximum link activation with cooperative transmission and interference cancellation in wireless networks," *IEEE Transactions on Mobile Computing*, vol. 16, no. 2, pp. 408–421, Feb. 2017.

[10] L. Shi, Y. Hu, J. Xu, Y. Shi, and X. Ding, "The mobile base station strategy for wireless networks with successive interference cancellation," *IEEE Access*, vol. 7, pp. 88 570–88 578, 2019.

[11] P.-T. de Boer, D. P. Kroese, S. Mannor, and R. Y. Rubinstein, "A tutorial on the cross-entropy method," *Annals of Operations Research*, vol. 134, no. 1, pp. 19–67, Feb 2005. [Online]. Available: https://doi.org/10.1007/s10479-005-5724-z

[12] M. Mozaffari, W. Saad, M. Bennis, and M. Debbah, "Unmanned aerial vehicle with underlaid device-to-device communications: Performance and tradeoffs," *IEEE Transactions on Wireless Communications*, vol. 15, no. 6, pp. 3949–3963, June 2016.

[13] D. Yuan, V. Angelakis, L. Chen, E. Karipidis, and E. G. Larsson, "On optimal link activation with interference cancelation in wireless networking," *IEEE Transactions on Vehicular Technology*, vol. 62, no. 2, pp. 939–945, Feb. 2013.

[14] *"Cisco Wireless Mesh Access Points, Design and Deployment Guide, Release 7.3 x"*, www.cisco.com, Aug. 2012. [Online]. Available: https://www.cisco.com/c/en/us/td/docs/wireless/technology/mesh/7-3/design/guide/Mesh.pdf

[15] A. B. Sediq, R. H. Gohary, R. Schoenen, and H. Yanikomeroglu, "Optimal tradeoff between sum-rate efficiency and jain's fairness index in resource allocation," *IEEE Transactions on Wireless Communications*, vol. 12, no. 7, pp. 3496–3509, July 2013.